San Miguel, V., Bochet, C. G. & del Campo, A. (2011): Wavelength-Selective Caged Surfaces: How Many Functional Levels Are Possible? *Journal of the American Chemical Society*, 133 (14), pp. 5380-5388.

Wavelength-Selective Caged Surfaces: How Many Functional Levels Are Possible?

Verónica San Miguel,[†] Christian G. Bochet,[‡] and Aránzazu del Campo*[,†]

[†]Max-Planck-Institut für Polymerforschung, Ackermannweg 10, 55128 Mainz, Germany

[‡]Department of Chemistry, University of Fribourg, Chemin du Musée 9, CH-1700 Fribourg, Switzerland

Corresponding Author delcampo@mpip-mainz.mpg.de

ABSTRACT: The possibility of wavelength-selective cleavage of seven photolabile caging groups from different families has been studied. Amine-, thiol-, and carboxylic-terminated organosilanes were caged with *o*-nitrobenzyl (NVOC, NPPOC), benzoin (BNZ),(coumarin-4-yl)methyl (DEACM), 7-nitroindoline (DNI, BNI), and *p*-hydroxyphenacyl (pHP) derivatives. Caged surfaces modified with the different chromophores were prepared, and their photosensitivity at selected wavelengths was quantified. Different pairs, trios, and quartets of chromophore combinations with wavelength-selective photoresponse were identified. Our results show, for the first time, the possibility of generating surfaces with up to four different and independently addressable functional levels. In addition, this manuscript presents the first systematic comparison of the photolytic properties of different photolabile groups under different irradiation conditions.

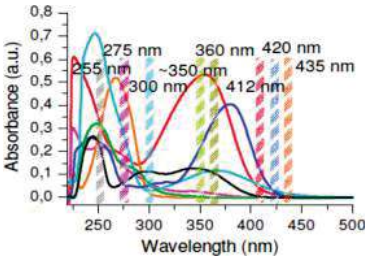

INTRODUCTION

Photolabile caged compounds[1] have been used over the last 30 years in cell biology to photoregulate the activity of different bioactive agents.[2] The biological activity of the caged compound is blocked because of the presence of a (in most cases) covalently bound chromophore. Light irradiation cleaves the chromophore and restores function. Using this approach defined concentration jumps of a bioeffector (i.e., Ca^{2+}, ATP, glutamate) have been generated in the cell culture medium within microseconds. More recently the activity of two different molecular species could be photoregulated independently based on the wavelength-selective response of two chromophores.[3] For this purpose, *o*-nitroveratryl esters have been used in combination with pivaloylpropanediol,[3e] 3,5-dimethoxybenzoin,[3c,h] (coumarin-4-yl)methyl,[3f,g,i] and derivatives upon single-[3] or two-photon[3g] excitation.

Compared to other external stimuli, light offers a precise spatiotemporal control of the activation step. For this reason, photolabile caged compounds have been used in the past few years to prepare chemically micropatterned surfaces based on surface layers containing caged chemical functionalities.[3h,i,4] Using masks or arrays of micromirrors for site-selective irradiation, reactive sites down to submicrometer size can be activated and used for subsequent attachment of other species. This strategy has been exploited to directly synthesize biomolecules at surfaces in an array format (microarrays) by means of iterative light-activation and monomer coupling cycles.[4b,5] Microarrays of peptides,[4b,6] oligonucleotides,[7] and peptoids[8] have been reported. Other species such as metallic nanoparticles,[9] polymer colloids,[3h,10] fluorescent dyes,[10,11] or biotinylated proteins[4e,12] have also been patterned using caged surfaces. We have used a similar approach to photoregulate cell adhesion and to obtain micropatterns of cells on different substrates.[4c] Bifunctional surfaces containing two types of chromophores have also been developed in our group and tested for site-selective immobilization of oligonucleotides and proteins.[3h,i,4a,4f,13] This is a particularly flexible approach, since a good number of photoremovable groups are known that could be combined with the different organic functional groups and applied to generate biosensors and cell-responsive surfaces with a great number of biochemically tunable states. However, this requires previous knowledge on the photoreactivity of the different chromophores across the absorption spectrum.

In this manuscript we report the wavelength-selective photolysis of seven surface-attached photoremovable groups that belong to different families. Caged organosilanes have been synthesized, and the resulting caged surfaces have been irradiated with different wavelengths and doses. Our results evidence the potential of this approach for generating photoactivatable surfaces with up to four independent functional levels that can be tuned with accurate spatial, temporal, and compositional resolution.

EXPERIMENTAL SECTION

Synthetic Procedure. All protocols for the synthesis of the photolabile derivatives (Scheme 1) and the preparation of the photosensitive surface layers are included as Supporting Information.

Scheme 1. Synthetic Route and Chemical Structure of Obtained Photosensitive Silanes

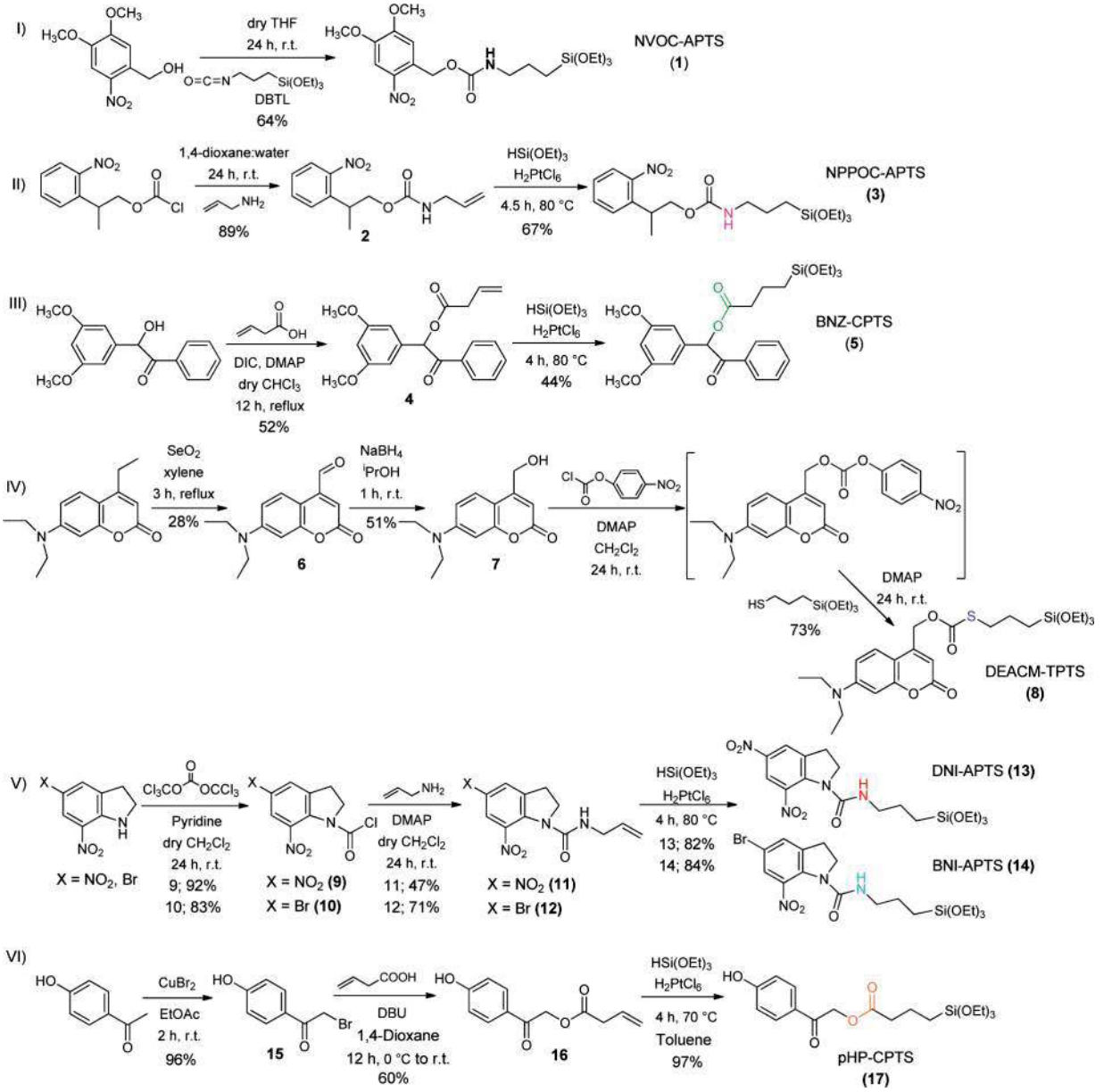

Characterization of Surface Layers. Chromophore concentration at the surface was followed by recording UV/vis spectra on quartz substrates. The surface density of the chromophore, Γ (molecs cm^{-2}), can be estimated from the UV absorbance using $\Gamma = {}^1/_2[A_\lambda \varepsilon_\lambda{}^{-1} N_A]$, where A_λ is the absorbance of the surface layer at a given wavelength, ε_λ is the molar extinction coefficient of the chromophore in solution at λ, and N_A is Avogadro's number.[14−17] The factor ${}^1/_2$ refers to the fact that the quartz slides are modified on both sides. Note that this calculation assumes that the molar extinction coefficients of the chromophores in solution and at the surface are the same. This is true only if anchored chromophore−chromophore or chromophore−surface interactions are disregarded.[14]

Photolysis Experiments at the Surface. Irradiation of the substrates was carried out using a Polychrome V system (TILL Photonics GmbH, Gräfelting, Germany) and a LUMOS 43 (Atlas Photonics Inc., Fribourg, Switzerland) as monochromatic light sources. The wavelengths and irradiances used with the Polychrome lamp were as follows: 345 nm (0.78 mW cm^{-2}), 350 nm (0.80 mW cm^{-2}), 358 nm (0.95 mW cm^{-2}), 366 nm (1.08 mW cm^{-2}), 412 nm (1.47 mW cm^{-2}), 420 nm (1.53 mW cm^{-2}), and 435 nm (1.60 mW cm^{-2}); and with LUMOS 43 were as follows: 255 nm (0.45 mW cm^{-2}), 275 nm (1.65 mW cm^{-2}), 300 nm (1.76 mW cm^{-2}), 360 nm (2.55 mW cm^{-2}), 420 nm (364 mW cm^{-2}), and 435 nm (262 mW cm^{-2}). After irradiation, substrates were sonicated in THF and rinsed with Milli-Q water before recording UV−vis spectra. Figure A in Supporting Information shows the UV spectra of the different lamps.

Calculation of the Photolytic Efficiency at Different Wavelengths (conversion and $\varepsilon_\lambda\phi$ product). The conversion of the photolytic reaction was calculated from the absorbance decay at λ_{max} measured by UV spectroscopy on modified quartz substrates after exposure with increasing dose and washing. The ratio of the

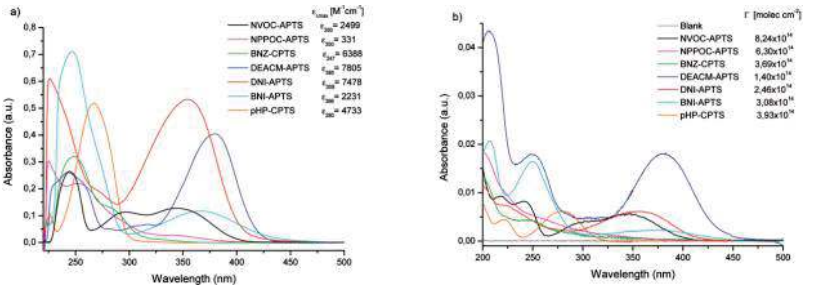

Figure 1. Comparative UV spectra of caged silanes in solution (a) and modified quartz surfaces (b).

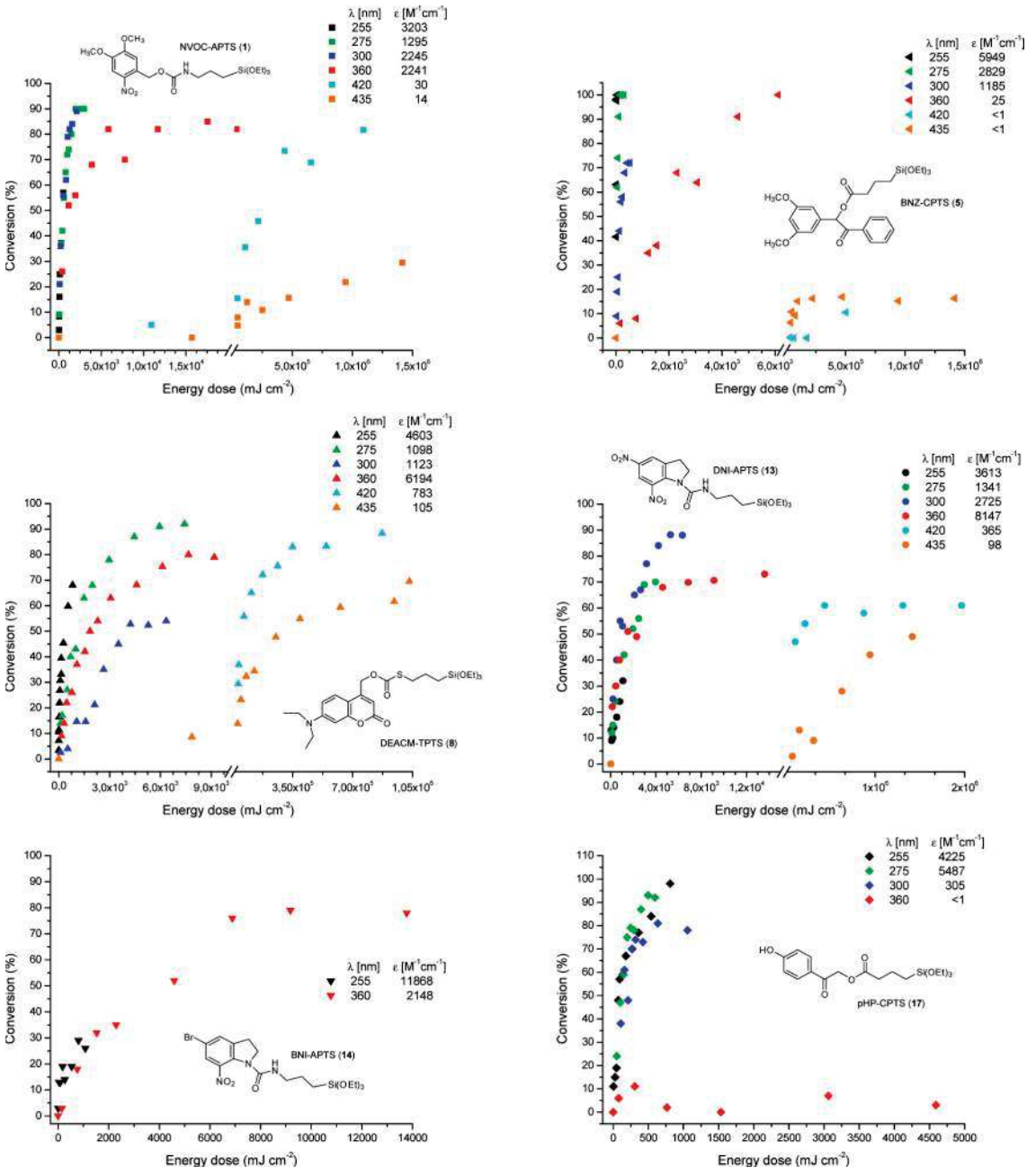

Figure 2. Photolysis conversion (%) versus irradiation dose of each chromophore at different wavelengths.

absorbance at λ_{max} after irradiation to the amount of initial absorbance multiplied by 100 gave the percent of chromophore remaining after exposure for a given time. From this, the conversion (%) upon exposure was found by subtraction for the different doses. The

Scheme 2. Schematic Mechanism of Photocleavage and Photolytic Products of Modified Surfaces with Caged Silanes

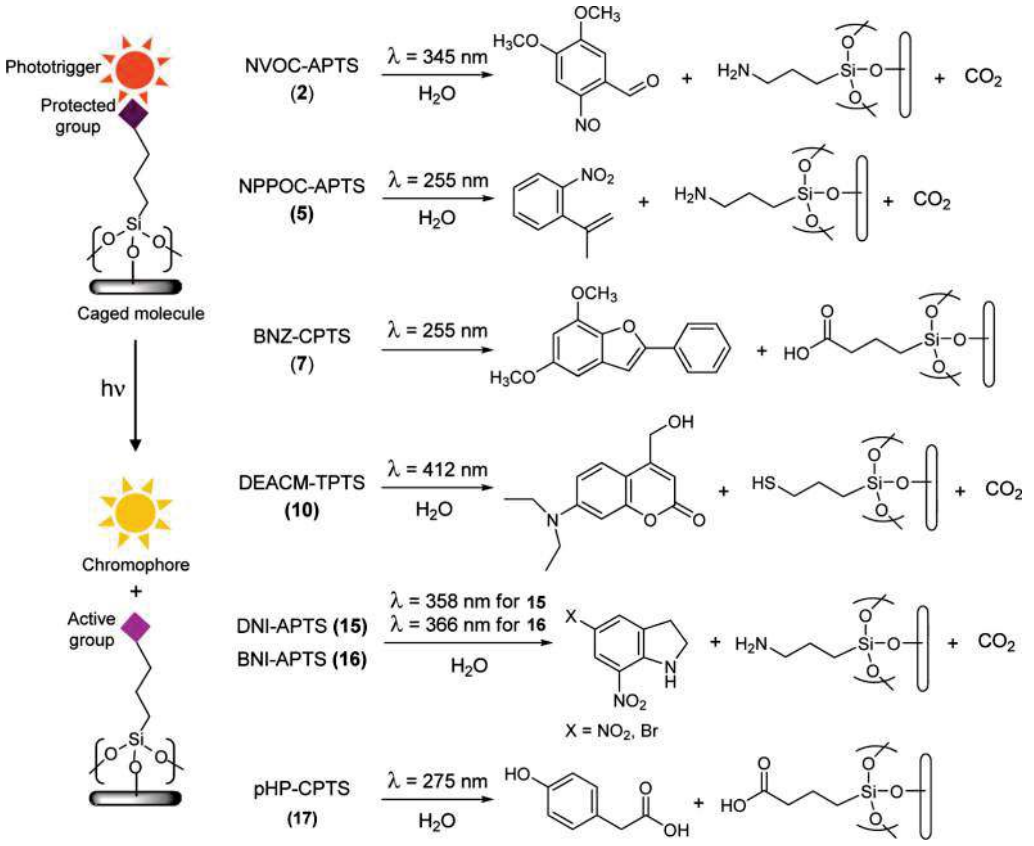

Table 1. Spectroscopic Data of Different Caging Groups and Caged Compounds in THF

chromophores	λ_{max} [nm]	absorption coefficient ($\varepsilon_{\lambda max}$) [$M^{-1}$ cm^{-1}]
nitroveratrol	346	7159
NVOC-APTS (**1**)	350	2499
NPPOC	340	457
2	340	471
NPPOC-APTS (**3**)	350	331
4	245	9979
BNZ-CPTS (**5**)	247	6388
7	365	17429
DEACM-TPTS (**8**)	385	7805
DNI	363	15710
11	357	13743
DNI-APTS (**13**)	358	7478
BNI	434	7068
12	366	3594
BNI-APTS (**14**)	366	2231
pHP	268	15993
16	267	9834
pHP-CPTS (**17**)	267	5988

product $\varepsilon_\lambda \phi$ for each exposure wavelength and chromophore was calculated by fitting the conversion curves to the photokinetic equation

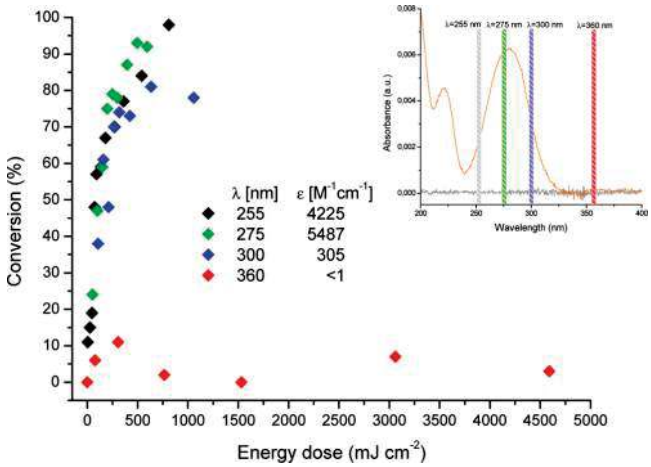

Figure 3. Conversion (%) of the photocleavage at the surface of the chromophore pHP-CPTS upon irradiation at different wavelengths and the UV spectrum of the corresponding silane (inset).

$$\frac{dx}{dt} = -I_0 \ln(10)\varepsilon_\lambda \phi x$$

which was specially developed for photolysis experiments at surfaces.[18] In this equation x represents the relative surface coverage of the photoreactive group, and I_0 is the illumination intensity in Einstein per units of time and area.

RESULTS

Amine, thiol, and carboxylic groups were caged with seven different chromophores belonging to five families: *o*-nitrobenzyl (NVOC, NPPOC), benzoin (BNZ), (coumarin-4-yl)methyl (DEACM), 7-nitroindoline (DNI, BNI), and *p*-hydroxyphenacyl (pHP). The photosensitive silanes **1**, **3**, **5**, **8**, **13**, **14**, and **17** were obtained and isolated in good yields following the synthetic route specified in Scheme 1. The detailed synthetic protocols are included as Supporting Information.

Figure 1a shows the UV−vis spectra of the photosensitive silanes in solution, and Table 1 compares the values of λ_{max} and the absorption coefficient of the silanes and their precursors. The caging reaction involves formation of a carbamate, carbonate, or ester bond. This modification does not significantly change the shape of the UV spectra of the chromophore, and the position of λ_{max} remains almost unchanged. Only BNI shows a 70 nm blue shift of the maximum, which is explained by the fact that the functionalization occurs directly on a conjugated functional group (aniline-type nitrogen). However, the caging step significantly decreases the absorbance of the chromophores by a factor of 2 to 3 times. It is important to note that a decrease in absorbance has a negative effect in the overall photolytic efficiency. The absorbance coefficient also decreases upon silanization. We do not have an explanation of these observations.

Figure 1b shows the UV spectra of the photosensitive silanes after reaction with the silica surface. The general profile of the UV spectra of the chromophores after surface attachment is similar to solution spectra. This suggests that the attached chromophores do not interact with the surface or within themselves, and therefore we do not expect surface-induced variations of the photochemical properties. From the absorbance values, and assuming the same absorbance coefficient of the chromophore at the surface and in solution, the surface density of chromophore can be estimated (see Experimental Section part for details). Values between 1.5 and 8×10^{14} molecs cm^{-2} were obtained, indicating a submonolayer surface coverage (note that surface density of a self-assembled monolayer of thiols on gold with maximum coverage[19] is 4.5×10^{14} molecs cm^{-2}, whereas DNA coverages on DNA chips are typically smaller[5b] and in the range between 10^{12} and 10^{13} molecs cm^{-2}). The spectra display significant differences in absorbance between the chromophores across the spectrum that can be exploited for chromatic selectivity. The following irradiation experiments address this question.

The modified substrates were exposed to light of selected wavelengths between 255 and 435 nm using two different light sources: a Xe-lamp coupled to a monochromator and a LED-based source (see Experimental Section for details). The photolytic reaction cleaved the chromophore from the surface (see Scheme 2), and the kinetics of the photolysis could be followed by the decay in the UV absorbance of the substrates after irradiation and a washing step (Figure B in Supporting Information shows the UV spectra of the substrates before and after full exposure at 255 nm). After full exposure (i.e., when longer irradiation did not further change the UV spectrum), almost no UV absorbance could be detected in pHP and BNZ substrates. However, a residual absorbance was visible for the other chromophores. The residual spectra show a profile different from that of the original one, indicating a change in the chemical structure of the surface-attached chromophore. This suggests that photolysis products remained attached (or trapped) to some extent to the surface layer. We hypothesized that the photoproducts may strongly interact with the surface and that their diffusion out of the dense surface layer may be hindered. In addition, side reactions may reattach reactive photolysis products to the surface (i.e., reaction of the aldehyde photoproduct with the free amines in NVOC).[3h] In fact, we soaked the substrates in different solvents for long periods of time prior to and after photolysis for facilitating diffusion of precursors out of the layer, and we used scavengers for capturing reactive byproduct, but none of these measurements reduced the residual absorbance. In summary, the measured spectra entailed two overlapping contributions: a major contribution from the remaining caged compound, and a minor contribution from photolytic products that remain attached to the surface layer. This is especially the case for the chromophores with a UV-absorbing byproduct such as nitroveratryl and nitroindoline derivatives.

From the recorded UV spectra, we calculated the amount of photocleaved chromophore upon exposure (conversion) from the ratio between the absorbance at λ_{max} before and after irradiation. Note that these values are subjected to two error sources. First, thin surface layers give low values of absorbance (typically <0.01) and the error in these measurements, especially at high conversions (i.e., low chromophore concentration at the surface) is ca. 15%. Second, we cannot subtract the contribution of the residual absorbance from the spectra, and therefore conversion values are underestimated (i.e., they represent the "worst" case).

Figure 2 shows the photolytic conversion of each chromophore upon exposure to different wavelengths and irradiation doses. The differences in the photosensitivity reflect the intensity of the absorption bands at the UV spectrum of the chromophore and, as expected, the photosensitivity of the chromophores is maximized when irradiating close to λ_{max}. Figure 3 shows the results for pHP cage together with its absorption spectrum to illustrate this point.

Figure 4 compares the photosensitivity of the different chromophores at a selected wavelength. This representation allows us to assess the potential and limitations of the chromophores for a wavelength-selective response. At 255 nm BNZ was fully photocleaved with low irradiation dose (1.1×10^2 mJ cm^{-2}) while all other cages remained stable under these conditions (but could be cleaved at higher doses). The comparative high efficiency of BNZ at this wavelength can be explained by its remarkably high ϕ (see Table B in Supporting Information for reported values of ϕ for the different chromophores). At 275 nm, BNZ was cleaved completely and pHP was cleaved up to 70% with doses up to 5×10^2 mJ cm^{-2} while the other cages were not affected significantly. The notable increase in efficiency of pHP from 255 to 275 nm correlates with the higher ε_{275}. pHP could be selectively cleaved at 275 nm against coumarin, nitroindoline, or dimethoxynitroveratryl families.

Irradiation at 300 nm cleaved all chromophores at comparable doses, and no selectivity could be detected. However, at ∼350 nm it was possible to cleave NVOC, DEACM, BNZ, and DNI up to 70% while pHP and BNI remained stable. It is important to note that NVOC, DEACM, BNZ, and DNI have their absorption maxima in this region while pHP does not absorb at $\lambda > 300$ nm and, therefore, remained stable against irradiation at longer wavelengths. Reported studies have found a low quantum yield of the photocleavage of BNI[15] (see Table B in Supporting Information), and this could be the reason for the low conversion in comparison to the other chromophores under

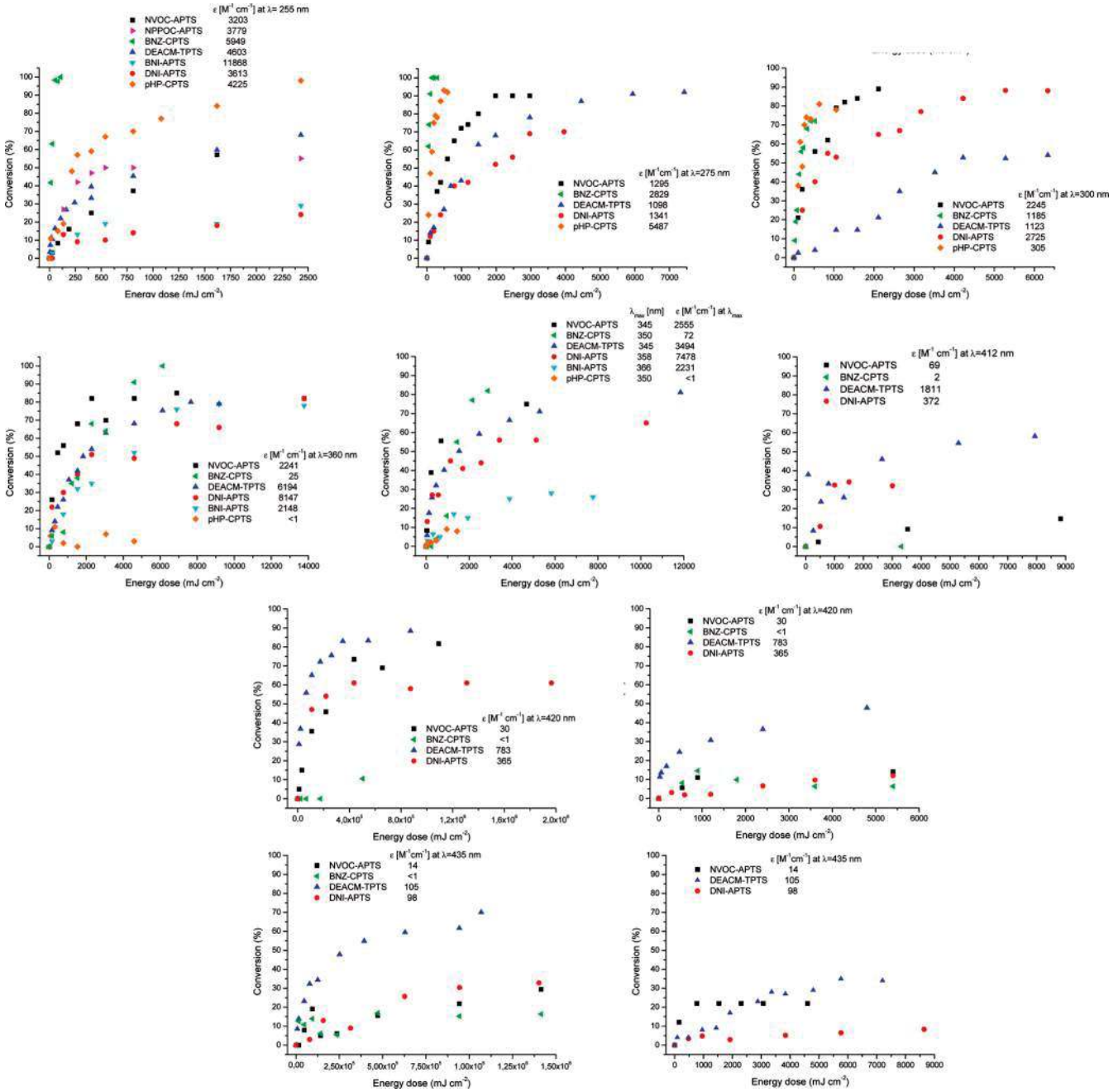

Figure 4. Conversion (%) of the photocleavage at the surface upon irradiation at different wavelengths.

these exposure conditions, even at a wavelength close to λ_{max}. In fact, irradiation at 360 nm with higher doses also cleaved BNI.

Irradiation at 412 nm cleaved DEACM and DNI up to 60% while NVOC and BNZ remained stable. At 420 nm NVOC, DEACM, and DNI cages reached their maximum photoconversion at a similar dose (4.2×10^5 mJ cm^{-2}), even though they presented a wide difference in ε_{420}. Obviously the change in the molar absorption coefficient is compensated by a change in the quantum yield. BNZ does not absorb in that region, and therefore it remained at the surface upon irradiation at wavelengths longer than 420 nm. Irradiation at 420 nm with a lower dose (4.8×10^3 mJ cm^{-2}) allowed the cleavage of DEACM up to 50% without affecting DNI and NVOC significantly. At 435 nm, DEACM could be differentiated and was cleaved up to 70%, while the other chromophores remained stable.

The photosensitivity is determined by the product of the absorption coefficient (ε_λ) and the quantum yield (ϕ) of the photolytic reaction at the given wavelength. We obtained the experimental value of the product $\varepsilon_\lambda\phi$ from the conversion curves by fitting them to a photokinetic equation modeling the special case of photolysis at surfaces (see ref 18 and Experimental Section part for more details). Table 2 presents the obtained values of $\varepsilon_\lambda\,\phi$ for the different caged compounds. It is important to highlight that these values are affected by the underestimated conversion values due to residual absorbance in the UV spectra (as stated before). This means that they should be regarded as orientative but not accurate, as it is typically assumed from solution experiments where the

Table 2. Calculated Values of the Product $\varepsilon_\lambda\phi$ for the Caged Organosilanes Obtained by Fitting the Experimental Conversion Data in Figure 4 Following the Photokinetic Equation from Ref 18[a]

cages	$\lambda_{irradiation}$ (nm)	$\varepsilon_\lambda\phi$ ($M^{-1}cm^{-1}$)
NVOC (**1**)	255	310
	275	504
	300	370
	345	380
	360	97
	412	43
	420	0.61
	435	0.30
NPPOC (**3**)	255	1167
BNZ (**5**)	255	8239
	275	4001
	300	1206
	350	263
	360	65
DEACM (**8**)	255	517
	275	136
	300	69
	345	135
	360	75
	412	126
	420	2.2
	435	0.91
DNI (**13**)	255	589
	275	221
	300	170
	358	128
	360	84
	412	237
	420	1.09
	435	0.27
BNI (**14**)	255	385
	366	89
	360	47
pHP (**17**)	255	540
	275	1379
	300	1473

[a] See Experimental Section and Table A in Supporting Information for more details.

contributions to absorbance from the photolysis products can be accurately determined. Because a direct measurement of ε_λ of the chromophore at the surface is not accessible, we cannot make an accurate estimation of ϕ (a rough estimation could be made by taking the value of ε_λ of the chromophore in solution included in Table A in Supporting Information).

The collection of data presented above was recorded by irradiating the modified (dry) substrate under ambient conditions. However, according to reported data on the photolysis of pHP, DEACM, DNI, and BNI in solution, the presence of protic solvents alters the photolytic mechanism, products, and kinetics.[2b] We performed the same experiments by irradiating the substrate immersed in a water-containing solution. No significant differences in the photolysis data could be observed

Table 3. Final Conversion Data (%) of the Photocleavage at the Surface for Silanes[a]

	caged silanes						
λ [nm] (E [mJ cm^{-2}])	NVOC (**1**)	NPPOC (**3**)	BNZ (**5**)	DEACM (**8**)	DNI (**13**)	BNI (**14**)	pHP (**17**)
255 (1.1×10^2)	⊗	50	100	⊗	⊗	⊗	57
255 (2.2×10^3)	57	55	100	68	32	30	98
275 (3.0×10^2)	37	--	100	⊗	⊗	--	60
275 (5.0×10^2)	55	--	100	27	24	--	92
300 (6.3×10^2)	60	--	72	⊗	50	--	81
300 (2.1×10^3)	89	--	72	21	65	--	81
~350 (2.9×10^3)	70	--	82	62	52	25	⊗
360 (6.1×10^3)	81	--	100	75	64	71	⊗
412 (4.5×10^3)	⊗	--	⊗	58	34	--	--
420 (4.2×10^5)	81	--	⊗	88	65	--	--
435 (6.3×10^5)	30	--	⊗	70	30	--	--

[a] Data reflect possible chromophore combinations for a wavelength-selective response. The symbol ⊗ indicates that the chromophore cannot be cleaved under the corresponding conditions. The symbol -- indicates that the photolysis experiment was not performed at that wavelength because, according to the results at neighboring wavelengths and the expected photosensitivity from the UV spectrum, no relevant wavelength sensitive response was expected.

(see Figure C in Supporting Information for data with DNI-APTS). It seems that adsorbed water on the surface layers as a consequence of air humidity acts as a protic solvent component for the photolysis.

DISCUSSION

We have demonstrated that photoremovable caging groups maintain their photochemical properties when attached to surfaces. Table 3 summarizes the values of the final conversion at full exposure for the different chromophores and wavelengths. According to these data, the following combinations of pairs, trios, and quartets have shown wavelength-selective responses within different spectral regions. The following list specifies the ones in which the cleavage of the chromophore is achieved at conversion values >70% (according to Table 3). The energy doses under which we have proofed the wavelength sensitivity appear in parentheses. This list proves that caged surfaces with up to four different functional levels can be obtained. Up to now only bifunctionality had been demonstrated.[3c,d,h,i]

Pairs:

(1) BNZ (**5**) at 255 nm (1.1×10^2)/NVOC (**1**) at 420 nm (4.2×10^5); orthogonal
(2) BNZ (**5**) at 255 nm (1.1×10^2)/DEACM (**8**) at 420 nm (4.2×10^5); orthogonal
(3) BNZ (**5**) at 255 nm (1.1×10^2)/DNI (**13**) at 420 nm (4.2×10^5); orthogonal
(4) DEACM (**8**) at 420 nm (4.2×10^5)/pHP (**17**) at 275 nm (5.0×10^2)
(5) pHP (**17**) at 300 nm (6.3×10^2)/DEACM (**8**) at 420 nm (4.2×10^5); orthogonal
(6) DNI (**13**) at 360 (6.1×10^3)/pHP (**17**) at 275 nm (5.0×10^2); orthogonal
(7) NVOC (**1**) at 360 (6.1×10^3)/pHP (**17**) at 275 nm (5.0×10^2)

(8) BNZ (**5**) at 360 nm (6.1×10^3)/pHP (**17**) at 275 nm (5.0×10^2)

Trios:

(9) DEACM (**8**) at 435 nm (6.3×10^5)/NVOC (**1**) at 420 nm (4.2×10^5)/BNZ (**5**) at 255 nm (1.1×10^2)

(10) DEACM (**8**) at 435 nm (6.3×10^5)/NVOC (**1**) at 360 nm (6.1×10^3)/pHP (**17**) at 275 nm (5.0×10^2)

(11) DEACM (**8**) at 435 nm (6.3×10^5)/DNI (**13**) at 420 nm (4.2×10^5)/BNZ (**5**) at 255 nm (1.1×10^2)

(12) DEACM (**8**) at 435 nm (6.3×10^5)/DNI (**13**) at 420 nm (4.2×10^5)/pHP (**17**) at 275 nm (5.0×10^2

(13) DEACM (**8**) at 435 nm (6.3×10^5)/BNZ (**5**) at 360 nm (6.1×10^3)/pHP (**17**) at 275 nm (5.0×10^2)

(14) NVOC (**1**) at 420 nm (4.2×10^5)/BNZ (**5**) at 360 nm (6.1×10^3)/pHP (**17**) at 275 nm (5.0×10^2)

(15) DNI (**13**) at 420 nm (4.2×10^5)/BNZ (**5**) at 360 nm (6.1×10^3)/pHP (**17**) at 275 nm (5.0×10^2)

Quartets:

(16) DEACM (**8**) at 435 nm (6.3×10^5)/NVOC (**1**) at 420 nm (4.2×10^5)/BNZ (**5**) at 360 nm (6.1×10^3)/pHP (**17**) at 275 nm (5.0×10^2)

(17) DEACM (**8**) at 435 nm (6.3×10^5)/DNI (**13**) at 420 nm (4.2×10^5)/BNZ (**5**) at 360 nm (6.1×10^3)/pHP (**17**) at 275 nm (5.0×10^2)

Not all combinations of cages are orthogonal, meaning that in the irradiation sequence one chromophore should always be cleaved before the other. Only the orthogonality between NVOC and BNZ had been proofed already and exploited in solution[3c] and surface experiments.[3h] Our results extend the number and wavelength range of orthogonal deprotection to five different combinations of cages (as indicated in the list).

For DEACM and BNZ, selective photocleavage was obtained by changing the energy dose using the same wavelength. Such intensity-selective uncaging could be important for sensing applications.

SUMMARY

We have analyzed the photolysis of seven different surface-attached photolabile groups at different wavelengths and identified spectral windows where the chromophores show different photosensitivities. Our results demonstrate that caged surfaces with up to four independently photoactivatable functional levels can be obtained using DEACM/NVOC and DNI/BNZ/pHP as chromophores and 435/420/360/275 nm as an irradiation sequence. An extension of the number of functional levels by using other caging families or two-photon excitation is a work in progress in our groups.

ACKNOWLEDGMENT

The authors thank José María Alonso and Gemma Rodríguez for previous work in this field and support in the synthetic protocols and also thank Michele Drechsler for support in the synthetic work. A.d.C. and V.S.M. thank DFG (Project CA880/3-1) for financial support.

REFERENCES

(2) (a) Mayer, G.; Heckel, A. *Angew. Chem., Int. Ed.* **2006**, *45*, 4900.(b) Goeldner, M.; Givens, R. *Dynamic Studies in Biology: Phototriggers, Photoswitches and Caged Biomolecules*; Wiley-VCH: Weinheim, 2005.

(3) (a) Blanc, A.; Bochet, C. G. *J. Org. Chem.* **2002**, *67*, 5567. (b) Bochet, C. G. *Tetrahedron Lett.* **2000**, *41*, 6341. (c) Bochet, C. G. *Angew. Chem., Int. Ed.* **2001**, *40*, 2071. (d) Bochet, C. G. *Synlett* **2004**, 2268. (e) Kessler, M.; Glatthar, R.; Giese, B.; Bochet, C. G. *Org. Lett.* **2003**, *5*, 1179. (f) Kotzur, N.; Briand, B.; Beyermann, M.; Hagen, V. *J. Am. Chem.Soc.* **2009**, *131*, 16927. (g) Kantevari, S.; Matsuzaki, M.; Kanemoto, Y.; Kasai, H.; Ellis-Davies, G. C. R. *Nat. Methods* **2010**, *7*, 123. (h) del Campo, A.; Boos, D.; Spiess, H. W.; Jonas, U. *Angew. Chem., Int. Ed.* **2005**, *44*, 4707. (i) Stegmaier, P.; Alonso, J. M.; del Campo, A. *Langmuir* **2008**, *24*, 11872.

(4) (a) Alonso, J. M.; Reichel, A.; Piehler, J.; del Campo, A. *Langmuir* **2008**, *24*, 448. (b) Fodor, S. P. A.; Read, J. L.; Pirrung, M. C.; Stryer, L.; Lu, A. T.; Solas, D. *Science* **1991**, *251*, 767. (c) Petersen, S.; Alonso, J. M.; Specht, A.; Duodu, P.; Goeldner, M.; Del Campo, A. *Angew. Chem., Int. Ed.* **2008**, *47*, 3192. (d) Pirrung, M. C.; Fallon, L.; McGall, G. *J. Org. Chem.* **1998**, *63*, 241. (e) Pirrung, M. C.; Huang, C. Y. *Bioconjugate Chem* **1996**, *7*, 317. (f) Stegmaier, P.; del Campo, A. *ChemPhysChem* **2009**, *10*, 357.

(5) (a) Fodor, S. P. A.; Rava, R. P.; Huang, X. H. C.; Pease, A. C.; Holmes, C. P.; Adams, C. L. *Nature* **1993**, *364*, 555. (b) Pirrung, M. C. *Angew. Chem., Int. Ed.* **2002**, *41*, 1277.

(6) Pellois, J. P.; Wang, W.; Gao, X. L. *J. Comb. Chem.* **2000**, *2*, 355.

(7) (a) McGall, G.; Labadie, J.; Brock, P.; Wallraff, G.; Nguyen, T.; Hinsberg, W. *Proc. Natl. Acad. Sci. U.S.A.* **1996**, *93*, 13555. (b) Pease, A. C.; Solas, D.; Sullivan, E. J.; Cronin, M. T.; Holmes, C. P.; Fodor, S. P. A. *Proc. Natl. Acad. Sci. U.S.A.* **1994**, *91*, 5022. (c) Gao, X. L.; Yu, P. L.; LeProust, E.; Sonigo, L.; Pellois, J. P.; Zhang, H. *J. Am. Chem. Soc.* **1998**, *120*, 12698. (d) Singh-Gasson, S.; Green, R. D.; Yue, Y. J.; Nelson, C.; Blattner, F.; Sussman, M. R.; Cerrina, F. *Nat. Biotechnol.* **1999**, *17*, 974. (e) McGall, G. H.; Barone, A. D.; Diggelmann, M.; Fodor, S. P. A.; Gentalen, E.; Ngo, N. *J. Am. Chem. Soc.* **1997**, *119*, 5081.

(8) Li, S. W.; Bowerman, D.; Marthandan, N.; Klyza, S.; Luebke, K. J.; Garner, H. R.; Kodadek, T. *J. Am. Chem. Soc.* **2004**, *126*, 4088.

(9) (a) Vossmeyer, T.; DeIonno, E.; Heath, J. R. *Angew. Chem., Int. Ed.* **1997**, *36*, 1080. (b) Vossmeyer, T.; Jia, S.; DeIonno, E.; Diehl, M. R.; Kim, S. H.; Peng, X.; Alivisatos, A. P.; Heath, J. R. *J. Appl. Phys.* **1998**, *84*, 3664.

(10) Jonas, U.; del Campo, A.; Kruger, C.; Glasser, G.; Boos, D. *Proc. Natl. Acad. Sci. U.S.A.* **2002**, *99*, 5034.

(11) (a) Millaruelo, M.; Eng, L. M.; Merting, M.; Pilch, B.; Oertel, U.; Opitz, J.; Sieczkowska, B.; Simon, F.; Voit, B. *Langmuir* **2006**, *22*, 9446. (b) Alvarez, M.; Best, A.; Pradhan-Kadam, S.; Koynov, K.; Jonas, U.; Kreiter, M. *Adv. Mater.* **2008**, *20*, 4563.

(12) (a) Sundberg, S. A.; Barrett, R. W.; Pirrung, M.; Lu, A. L.; Kiangsoontra, B.; Holmes, C. P. *J. Am. Chem. Soc.* **1995**, *117*, 12050. (b) Lee, K. N.; Shin, D. S.; Lee, Y. S.; Kim, Y. K. *J. Micromech. Microeng.* **2003**, *13*, 18.

(13) Á lvarez, M.; Best, A.; Unger, A.; Alonso, J. M.; del Campo, A.; Schmelzeisen, M.; Koynov, K.; Kreiter, M. *Adv. Funct. Mater.* **2010**, *20*, 4265.

(14) Bramblett, A. L.; Boeckl, M. S.; Hauch, K. D.; Ratner, B. D.; Sasaki, T.; Rogers, J. W. *Surf. Interface Anal.* **2002**, *33*, 506.

(15) Caruso, F.; Kurth, D. G.; Volkmer, D.; Koop, M. J.; Muller, A. *Langmuir* **1998**, *14*, 3462.

(16) Li, D. Q.; Swanson, B. I.; Robinson, J. M.; Hoffbauer, M. A. *J. Am. Chem. Soc.* **1993**, *115*, 6975.

(17) Tang, T. J.; Qu, J. Q.; Mullen, K.; Webber, S. E. *Langmuir* **2006**, *22*, 26.

(18) Woll, D.; Walbert, S.; Stengele, K. P.; Albert, T. J.; Richmond, T.; Norton, J.; Singer, M.; Green, R. D.; Pfleiderer, W.; Steiner, U. E. *Helv. Chim. Acta* **2004**, *87*, 28.

(19) Love, J. C.; Estroff, L. A.; Kriebel, J. K.; Nuzzo, R. G.; White-sides, G. M. *Chem. Rev.* **2005**, *105*, 1103.